

Physiochemical Characteristics of Solid Electrolyte Membranes for High-Temperature PEM Fuel Cell

M. A. Haque^{1,2,}, A. B. Sulong^{1,3 *}, E. H. Majlan¹, K. S. Loh¹, T. Husaini¹, R. Rosli¹*

¹ Fuel Cell Institute, Universiti Kebangsaan Malaysia, UKM Bangi, 43600, Selangor, Malaysia

² Department of Applied Chemistry and Chemical Engineering, Islamic University, Kushtia-7003, Bangladesh

³ Department of Mechanical and Materials Engineering Universiti Kebangsaan Malaysia, UKM Bangi, 43600, Selangor, Malaysia

*E-mail: ahsan.chem38@gmail.com, abubakar@ukm.edu.my

Received: 1 August 2018 / Accepted: 16 September 2018 / Published: 30 November 2018

Proton exchange membrane fuel cell (PEMFC) is one of the most promising clean energy conversion devices, whereas polybenzimidazole (PBI) polymer consider the potential electrolyte membrane for high temperature. In this study, solid polymer electrolyte membranes were studied the physiochemical occurrences such as proton conductivity, ion transfer number, oxidative stability, tensile strength, TGA, and FTIR analysis. The PBI copolymer-1 was shown the maximum proton conductivity (6.52 mS/cm) and ion transfer number (0.9723) compared with the PBI copolymer-2 and Nafion specimens. Based on AFM results, the PBI copolymer-1 had low surface roughness and remarkable grain number which favorable for ion conductivity. Despite that, it had excellent chemical stability in terms of Fenton solution and maximum weight loss measured at 4.5% after treated 200 h. The PBI copolymer-1 had high thermal and mechanical strengths that demonstrated in tensile test and TGA analysis. Moreover, acid doped solid electrolyte membranes were successfully demonstrated in single cell, which exhibited at 99.75 mW/cm² power density that can be recommended as a proton exchange membrane for high-temperature PEMFC application.

Keywords: Polybenzimidazole, Acid doping, Nyquist plot, Ion transfer number, Fenton test

1. INTRODUCTION

Nowadays, green energy is the most desirable all over the world to protect the earth. Because, we need to consider not only the limited reserves of fossil fuel for use in the future but also the question of CO₂ emission, which is directly correlated with global warming. According to the aforementioned issues, several research groups [1, 2] were suggested that the PEMFC is becoming the most popular and

alternative clean energy conversion device in the near future to use in automotive, stationary, and portable applications. In PEMFC, the proton exchange membrane is separated by the anode and cathode, which applied between the conduction of protons from one side to the other electrode side. Therefore, the expected proton conduction rate through the membrane is very effective for overall cell performance. At present, many of researchers [3, 4] are involving in the polymer electrolyte membranes development for PEMFC applications.

In a low operating temperature (usually < 80 °C) PEMFC, the perfluoro sulfonic acid (PFSA, Nafion) polymer membrane is commonly used as the electrolyte membrane due to its low ionic conductive resistance. Despite that it has some challenges, such as being expensive, having a limited working temperature, dependent on humidity, and inadequate for longer cell operations [5]. In high operating temperatures (usually 120–180 °C), the Nafion membrane acts like a nonconductive, because the dryness of conduction medium of proton exchange membrane at that temperatures. To solve these complexities, several research groups [6, 7] were introduced high thermo-chemical stable alternative polymeric membranes such as polyimides, polysulfones, polybenzoxazoles, PBI (polybenzimidazole), AB-PBI, poly(2,5-benzimidazole), poly(2,2-m-(phenylene)-5,5 bibenzimidazole), pyridine-based PBI, and sulfo-based PBI, preferable for use in high temperature PEMFC applications. The chemical structure of PBI and Nafion membranes are following as shown in Figure 1.

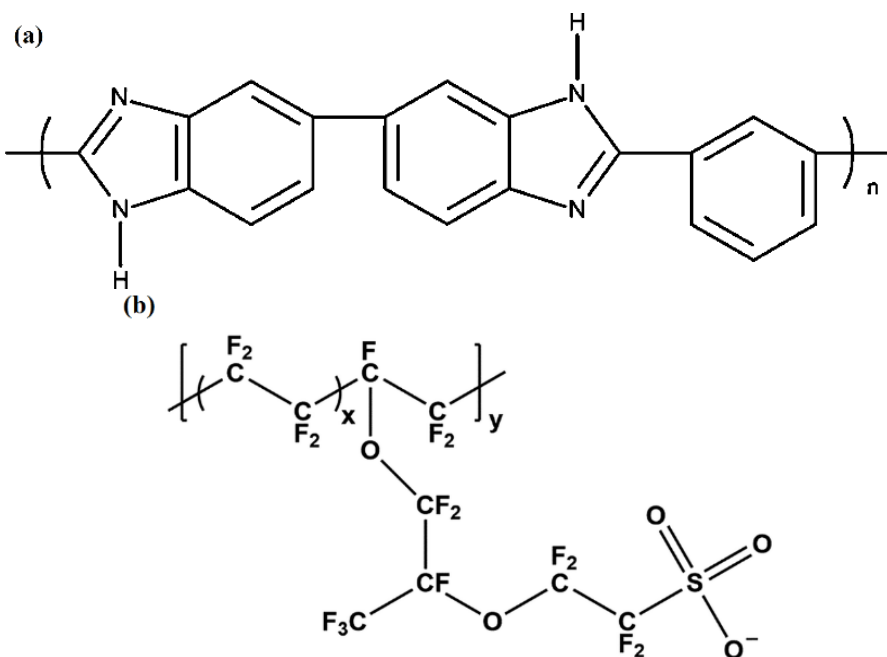


Figure 1. The chemical structure of (a) polybenzimidazole and (b) Nafion.

PBI-based membranes have some potential advantages compared with Nafion in terms of price, thermal, mechanical, and chemical properties. Moreover, the pristine PBI membrane has a low ionic conductivity due to insufficient conduction media for proton transportation. It is only able to manage a high proton conduction system whenever the membrane has required amount of acid doping level (ADL). The PBI membranes are basic in nature because of having the N-H sites in imidazole group [8].

Despite that this type of membrane could easily be improved by the treatment of strong acids such as H₃PO₄, H₂SO₄, HCl, HNO₃, HClO₄, and so on in order to enhance the proton conductivity. Phosphoric acid (H₃PO₄) is the most promising candidate for proton conduction media of solid polymer electrolyte membranes [9]. However, the excess acid doping that might be counterintuitive on the mechanical and thermal properties of the PBI membrane. Therefore, it is necessary to optimize the ADL of the PBI membrane to retain the prior criteria. In this research, the emphasis has been placed on the modification by the H₃PO₄ treatment as well as physiochemical characterization of the pristine solid electrolyte membranes.

2. MATERIALS AND METHODS

Pristine PBI polymer electrolyte membranes were purchased from the Fumatech BWT Group (Germany) and Nafion membrane supplied by the DuPont (USA). The chemical reagents, such as ortho-phosphoric acid, H₂O₂, and FeSO₄, were purchased from Sigma Aldrich (USA). All chemicals were in analyzed grade.

Pristine PBI polymer electrolyte membranes have to requisite a less volatile solvent with a high boiling point to support the conduction media, which may increase the hoping of hydrogen bonds inside the membrane. A research group [10] was explained the Grothious mechanism in their review article that was most likely to favor the proton transportation through the membrane. The PBI polymer membranes were cut into small pieces and submerged in the ortho-phosphoric acid bath (85 % conc. H₃PO₄) to acquire the expected proton conductivity. Prior to the acid doping, all membranes were dried in a vacuum oven at 110°C till a constant weight was reached. Later, the membrane thickness was measured by the Mitutoyo-7321 (Japan) thickness gauge. In addition, the membranes were dipped into acid bath for 3-4 days at ambient temperature. The membrane thickness was increased due to the gradual penetration of acid molecules inside the membrane. Moreover, the acid doped membranes were swept by lab tissue to remove any unexpected residue, and again dried for overnight at 70°C. Prior the proton conductivity measurement of Nafion, it was immersed in DI water to make sure proton conduction media.

The proton conductivity of all prepared membranes were measured by the Autolab Potentiostat (AUT84976) in context to the electrochemical impedance spectroscopic (EIS) analysis. The frequency ranges were used from 0.10 Hz to 1MHz, amplitude 0.01 V, and the applied current range 100 nA to 1 A. Using the 50 integration with the above parameters, it formed a Nyquist plot that was used to calculate the electrolyte resistance of that membrane. In this case, two Pt mesh probes were used to measure the proton conductivity through the membrane, according to the following equation (1) [11, 12].

$$\sigma = L/R_s A \quad (1)$$

whereas, σ is the proton conductivity (S/cm), L is the thickness of membrane (cm), R_s is the resistance of membrane (Ω), A is the membrane area πr^2 (cm²) and r is the radius of sample specimen.

It can be calculated the acid doping level (ADL) of doped PBI membranes based on the ion exchange capacity (IEC) technique [13, 14]. In this method, the acid doped membranes were immersed in 2.0 M NaCl solution and kept over-night for H⁺ ion exchange from the doped membrane. The resultant NaCl solution was titrated by a 0.02 M NaOH solution. The Phenolphthalein indicator was used to detect the end point. The membranes were titrated again and kept in a 1.0 M HCl solution for several hours. Later, it was dried in an oven at 105°C until the constant weight was obtained. Therefore, the ADL of the doped membrane was calculated according to the following equation (2) [15, 16].

$$ADL = V_{NaOH} * S_{NaOH} / W_{membrane} \quad (2)$$

whereas, V_{NaOH} is the volume of NaOH in ml, S_{NaOH} is the strength of NaOH in Molarity and $W_{membrane}$ is the dry weight of solid electrolyte membrane.

The most important and simple technique used to calculate for ion transfer number by the Wagner's Polarization [17]. Based on this idea, the current variation was measured in terms of time progress through the polarization at electrode-electrolyte interface. Theoretically, ion transfer number and electron transfer number are commonly unity. Therefore, the ion transfer number was calculated by the following equation (3).

$$t_i = I - I_s / I_t \quad (3)$$

whereas, t_i is the ions transfer number, I_s is the current on saturation (electronic current only) and I_t is the total current (ionic and electronic) at starting time (t=0).

The Fenton test was performed by the Fenton solution (4.0 % of H₂O₂, containing 4ppm of Fe²⁺ ions). The oxidative stability of the membrane is considered the how much weight loss % of the chemical treated membrane. The dried pristine PBI membranes were dipped into the Fenton solution at 70°C temperature under different time exposure, such as 40 h, 80 h, 120 h, 160 h, and 200 h and recorded the percentages (%) of weight loss. Later, the membranes were thoroughly washed with DI water and dried in a vacuum oven at 105°C for 6 hours before being weighed again [18, 19].

Several research groups [20, 21] were measured the mechanical strength of polymer electrolyte membranes by the tensile tester. In this case, above mentioned polymer electrolyte membranes were measured through the universal tensile tester machine (Instron 5567) by 30 N load cell at ambient temperature. The sample dimensions were 80 mm x 10 mm and kept at the speed rate of 5mm/min. All samples were conditioned at room temperature for 2 days prior the test.

The AFM (atomic force microscopy) images were measured by a commercial AFM system (model: NX-10; brand: Park system; South Korea). All images were taken at 5 μm × 5 μm scan area and the non-contact image processing mode. The silicon cantilever was used in the AFM system [22].

The thermal stability of PBI polymers be able to measure by the thermogravimetric (TGA) analysis [23]. Therefore, the membranes were analyzed within a temperature range of 50 to 700°C under isothermal heating conditions of 10 mL min⁻¹ of N₂ gas purging rate, and 10 min⁻¹ heating rate with the help of the Perkin-Elmer (STA6000) instrument. The FTIR (Fourier transform infrared spectroscopy) of PBI copolymer-1, PBI copolymer-2 and Nafion membranes were performed by the Perkin-Elmer FTIR instrument (Spectrum 400 FT-IR/FT-NIR, UK) in the range of 700 to 4000 cm⁻¹.

The MWCNT/Pt catalyst was dissolved in aqueous solution of isopropyl alcohol (60 vol. %). The Nafion solution (10 wt. %) also added in the catalyst loaded isopropyl alcohol solution which was sonicated (Model: Elma/E30H) for 30 minutes to acquire homogenous catalyst solution. The catalyst loading was conserved at 0.5 mg/cm^2 and 0.7 mg/cm^2 for anode and cathode electrodes, respectively.

This catalyst ink was deposited onto the gas diffusion layer (carbon paper; GDS 3250) by direct spray technique using the spray gun (Model: Sparmax GP35) which driven by the nitrogen gas flow. The spraying was conducted in a zigzag manner while the deposition rate was 0.3 ml/min. to 0.5 ml/min. The solid electrolyte membranes were sandwiched between two electrodes; anode and cathode. The membrane electrode assembly (MEA) was fabricated using the hot-press machine which deployed at 550 psi pressure with 3 minutes under 120°C temperature [24, 25, 26].

3. RESULTS AND DISCUSSION

3.1 Proton conductivity

Proton conductivity is the most selective criterion of solid polymer electrolyte membrane for PEM fuel cell. The Nyquist plot is familiarized to measure the proton conductivity of polymer electrolyte membranes based on the EIS technique. Figure 2(a), 2(b) and 2(c) show the Nyquist plots for the Nafion, PBI copolymer-1 and PBI copolymer-2 polymer electrolyte membranes, respectively. At high frequency range, it was appeared a small semicircle in these plots. Figure 2(d) also represents the equivalent circuit [$R_s(C[R_{ct}Q])$] for the respective Nyquist plots that reported our previous article [27]. Leong [28] showed that the phase angle was close to zero on that stage. From the equivalent circuit components, the conductance (C) and constant phase element (Q) are negligible impedance, because of the impedance is inversely proportional to the frequency. In addition, R_s and R_{ct} are also representing the ionic resistance and charge transfer resistance of the membrane. Moreover, the semicircle shape decreased and gradually shifted from lower frequency to the higher frequency region, at high temperature. Because, the R_s value (electrolyte resistance) was decreased with increase in temperature. In addition, the electrolyte resistance of Nafion, PBI copolymer-2 was a little bit higher than the PBI copolymer-1 membrane. Therefore, the PBI copolymer-1 membrane was low electrolyte resistance at high temperature compared with other membranes.

The conductivity of membrane was calculated by putting the value of electrolyte resistance (R_s), corresponding membrane area (A), and thickness (L), in equation (1). In case of Nafion, the conductivity was gradually increased in terms of temperature and the maximum ionic conductivity measured at 5.29 mS/cm . In contrast, it was significantly decreased the proton conductivity due to the dehydration of membrane at high operating temperatures. However, the proton conductivity was consecutively increased until 150°C temperature and observed the maximum at 6.52 mS/cm and 5.69 mS/cm for the PBI copolymer-1 and PBI copolymer-2 membranes, respectively.

The phosphoric acid has high possibility to change the pyrophosphoric acid at high temperature which is less conduction than the prior one. Therefore, it was reduced the proton conductivity at 175°C temperature of both PBI membranes. Moreover, the PBI copolymer-1 showed the highest conductivity than PBI copolymer-2. Because, the PBI copolymer-1 membrane was absorbed the maximum ADL

content compared with PBI copolymer-2 membrane which was accelerated by the conduction medium at high temperature.

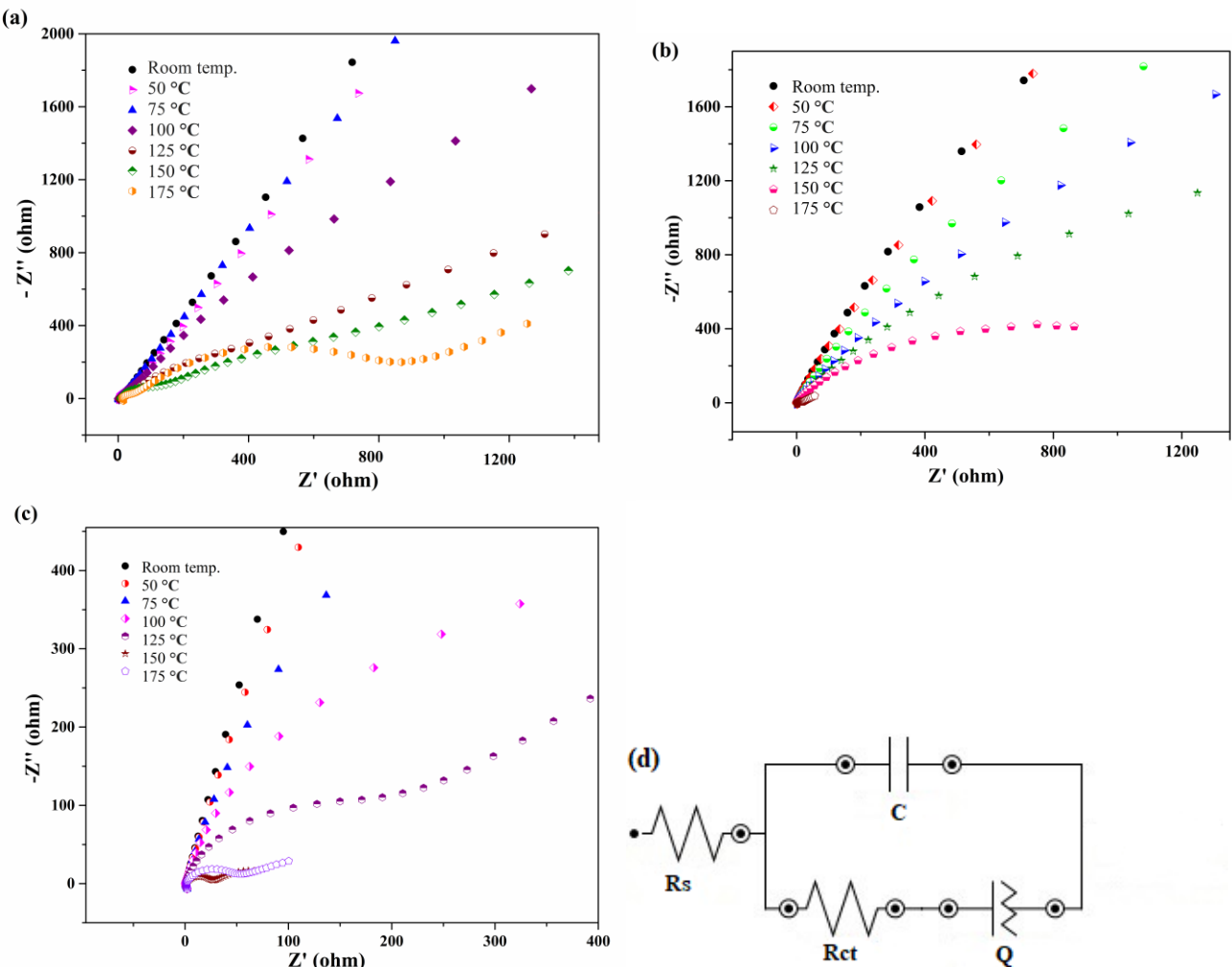


Figure 2. The Nyquist plot of (a) Nafion, (b) PBI copolymer-1, (c) PBI copolymer-2 membranes respectively, and their (d) equivalent circuit fitting.

Table 1 shows the various comparisons of solid electrolyte membranes for a similar application of proton conductivity. From the table, it is clearly seen that the PBI copolymer in this study was in good agreement with previous studies. Proton conductivity hugely depends on the ADL content and operating conditions such as temperature, percentage of relative humidity (% RH). S.W. Chuang [29] measured the proton conductivity at 3.0 mS cm^{-1} of acid doped PBI based membrane while ADL content was 11 mol/repeating unit at 160 °C temperature with the anhydrous condition. At similar conditions, it has been measured the proton conductivity at 6.52 mS cm^{-1} and 5.69 mS cm^{-1} of acid doped PBI copolymer-1 and PBI copolymer-2 during in this study. This development was achieved due to properly demonstrate of the acid curing process of proton exchange membranes.

Table 1. A comparison of acid doped PBI based solid electrolyte membranes for HT-PEMFC [10].

Membrane type	ADL	Temp. & % of RH	Conductivity	References
H ₃ PO ₄ -PBI copolymer-1	11.2 mol/repeating unit	150 °C ; anhydrous condition	6.52 mS cm ⁻¹	This work
H ₃ PO ₄ -PBI copolymer-2	11.0 mol/repeating unit	150 °C ; anhydrous condition	5.69 mS cm ⁻¹	This work
H ₃ PO ₄ -PBI/Im	11 mol/repeating unit	160 °C; anhydrous condition	3.0 mS cm ⁻¹	[29]
H ₃ PO ₄ -PBI	5.6 mol/repeating unit	200 °C; anhydrous condition	0.068 S cm ⁻¹	[30]
H ₃ PO ₄ -ABPBI	3.0 mol/repeating unit	180 °C; anhydrous condition	0.015 S cm ⁻¹	[31]
H ₃ PO ₄ -PBI	18.0 mol/repeating unit	180 °C; dry air	0.10 S cm ⁻¹	[32]
H ₃ PO ₄ -CsPOM/PBI	120 % mol	150 °C; 8.4 % RH	0.15 S cm ⁻¹	[33]
H ₃ PO ₄ -PTFE/PBI	300 % mol	180 °C; 8.4 % RH	0.30 S cm ⁻¹	[34]
H ₃ PO ₄ -PBI	300 % to 1600 % mol	160 °C; anhydrous condition	0.13 S cm ⁻¹	[35]
H ₃ PO ₄ - <i>p</i> PBI	29 mol/repeating unit	150 °C; anhydrous condition	0.16 S cm ⁻¹	[36]
H ₃ PO ₄ - <i>p</i> PBI	8.8 mol/repeating unit	180 °C; 1 % RH	0.15 S cm ⁻¹	[37]
H ₃ PO ₄ -PBI	11.0 mol/repeating unit	160 °C ; without humidity	0.14 S cm ⁻¹	[38]
H ₃ PO ₄ -PBI	20.4 mol/repeating unit	160 °C to 200 °C	0.20 S cm ⁻¹	[39]
H ₃ PO ₄ -PyPBI	8.5 mol/repeating unit	160 °C to 200 °C	0.10 S cm ⁻¹	[39]
H ₃ PO ₄ -ABPBI	3.1 mol/repeating unit	140 °C; 20% RH	80 mS cm ⁻¹	[40]

3.2 Ion transfer number

The initial current (when, t =0) to final current (when, t =5000 s) were taken at constant voltage (0.5 V) applied on the polymer electrolyte membrane specimens. In this case, instantaneous current was measured at ambient temperature and pressure with every interval of a minute. The variation of current was recorded in terms of time exposure for the Nafion, PBI copolymer-1 and PBI copolymer-2 membranes are shown in Figure 3. The applied direct current (*dc*) potential has migrated the ions towards the respective electrodes resulting in an ionic current. At the initial stage, the ionic current and electronic current, both were responsible for the total current. As being time progress, the ionic current was gradually suppressed because of the polarization of ions at the electrode surface area and finally stabilized the electronic current. In this study, the ion transfer number was found at 0.9705, 0.9723 and 0.9692 for the Nafion, PBI copolymer-1 and PBI copolymer-2, respectively. Although these values were indicated that all electrolyte membranes are ionic conductive, but the PBI copolymer-1 was a little bit higher than others. However, the results of ion transfer number was found an agreement with the proton conductivity of membranes.

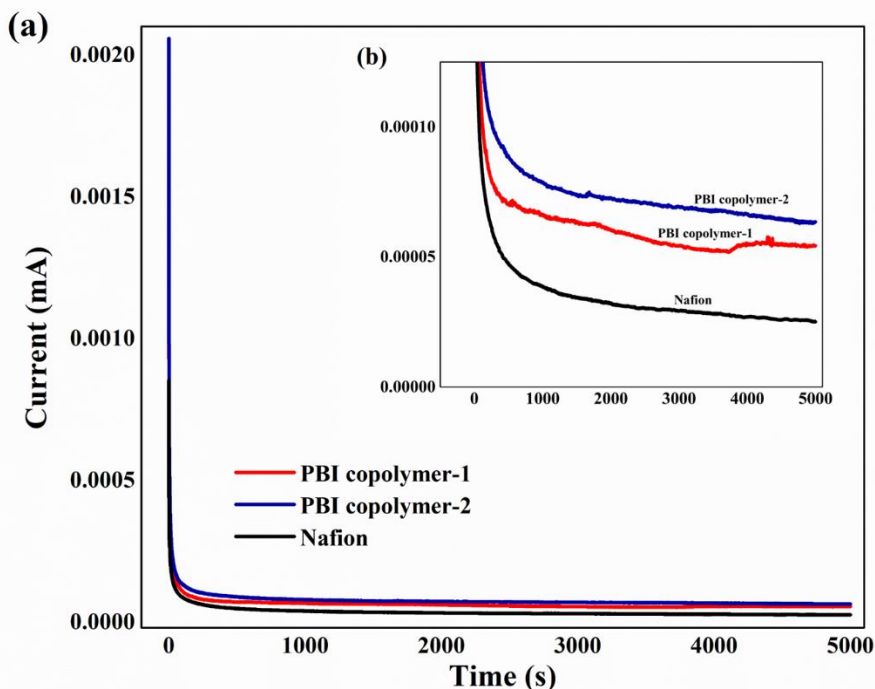


Figure 3. (a) An analysis of ion transfers number of membranes and (b) zoom in of (a).

3.3 Oxidative strength

The exothermal combustion of hydrogen and oxygen gasses leads to pinhole formation inside the membrane and accelerates the structural damage. During the operation mode such as open circuit voltage (OCV), low humidity, start-up, and down cycles are preferable to form H_2O_2 . Later, this decomposes into peroxide (HO^*), hydrogen peroxide (HOO^*), and reactive radicals. In addition, the incomplete oxidation reaction of fuel combustion makes for the reactive situation of a membrane, which is suitable for reactive radical compounds such as peroxide (HO^*) and hydrogen peroxide (HOO^*). Wu [41] showed that these reactive radicals are mainly responsible for the polymer electrolyte membrane degradation. Similarly, the weak bond of the membrane side such as the polymer side chain is predominantly attacked by the peroxide radicals, which leads to membrane degradation. The PBI copolymer-1 and PBI copolymer-2 membranes were immersed in a strong oxidizing agent of 4.0% H_2O_2 solution containing 4 ppm of Fe^{2+} ions at 70°C for measuring the polymer degradation. The membranes were oxidized gradually along with different exposure times and measured the weight loss %, which tell us the chemical stability of it.

From the Figure 4, it is clearly seen that the polymer degradation increases while extending the exposure time. The PBI copolymer-1 membrane was exhibited better chemical stability than the PBI copolymer-2. The maximum weight loss was found at 4.5 % and 4.9 % after treated 200 h by the H_2O_2 solution for the PBI copolymer-1 and PBI copolymer-2 membranes, respectively.

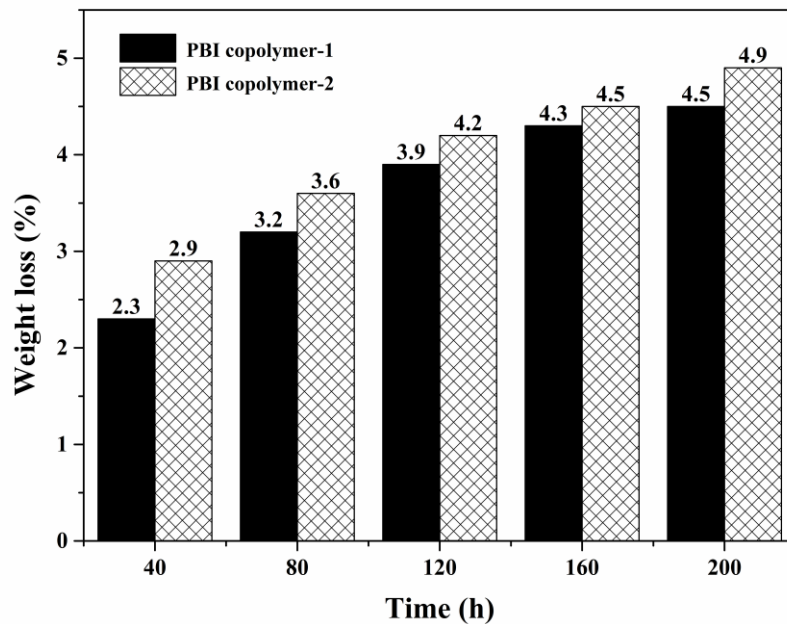


Figure 4. The chemical stability of PBI copolymer-1 and PBI copolymer-2 membranes.

Yang [38] reported that Nafion 115 weight losses at 5.0 % by the treatment of Fenton solution. In addition, high molecular weighted and cross-linked polymer membranes showed high chemical stability due to their long chain and chain rigidity which refers to the stiffness of the polymer. Liao [42] explained that the N-H group of a bulk polymer has been associated with vibration stretching that indicates the minimum degradation during radical oxidation of the membrane. However, the N-H group of PBI membranes is a little basic in nature that might neutralize under an acidic medium whenever acid doping of PBI membranes is carried out, and therefore stabilize the peroxide radicals.

3.4 Tensile strength

The tensile strength was measured of untreated and treated of Nafion and PBI membranes, at ambient temperature. Absorbed acid has a significant effect on the mechanical strength of the PBI membrane. A typical stress-strain curve is shown in Figure 5, and the maximum stresses were 215 MPa, 1338 MPa, and 1219 MPa in terms of their respective strains were 58.0 %, 13.7 % and 4.9 % for the Nafion, PBI copolymer-1 and PBI copolymer-2 membranes, respectively. Based on that illustration, it is the big mechanical differences between the untreated and acid doped of both PBI copolymer-1 and PBI copolymer-2 membranes. Xiao [39] showed that high ADL is directly correlated with the plasticizing effect on the both PBI copolymer-1 and PBI copolymer-2 polymer membranes. Therefore, high ADL is responsible for high plasticity properties in the polymer. In case of acid doped PBI copolymer-1 and PBI copolymer-2 membranes, the elongations were improved due to the plasticizing effect, that noted as 42.8%, and 16.6 %, as well as their stability were 685 MPa and 506 MPa. Yang [38] reported that mechanical strength does not depend on the ADL but it also relates to the molecular weight of a polymer and operating temperature. A high molecular weight polymer displays more stiffness than

the low molecular weight polymer, because of its having high bonding strength, which represents high tensile strength. However, a high working temperature is lowering the mechanical strength of a polymer membrane.

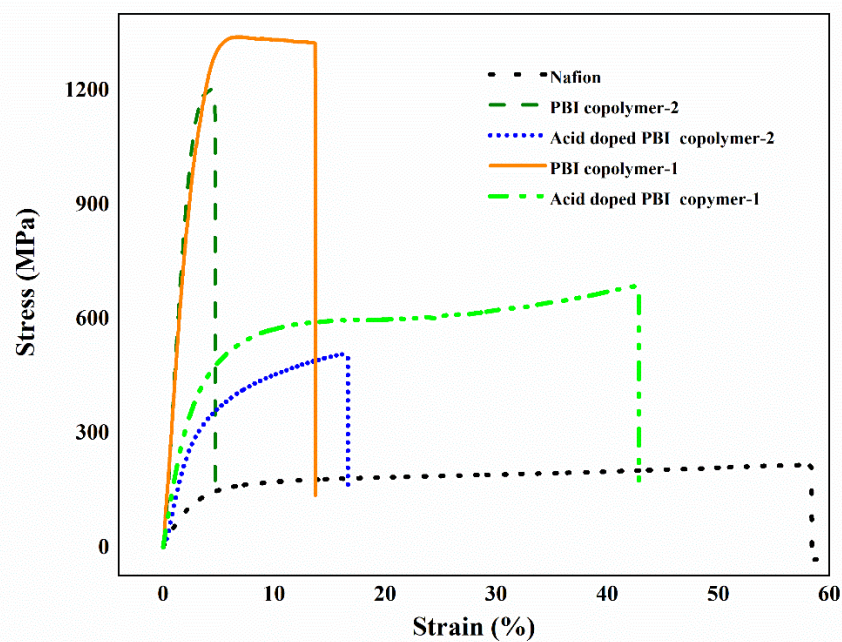


Figure 5. Stress-strain curve of Nafion, PBI copolymer-1 and PBI copolymer-2 membranes.

3.5 Thermal properties

The thermal properties have been investigated by the TGA analysis as shown in Figure 6. According to the TGA curve, the Nafion, PBI copolymer-1 and PBI copolymer-2 (pristine or acid doped) membranes were weight lost in two more stages. Initially, it was reduced a small amount of % weight due to the evaporation of water and residual solvents, especially the H₃PO₄ acid contents present either the PBI copolymer-1 or PBI copolymer-2 membrane. From the figure, it has seen that 3% to 4% of weight loss for all specimens until 150°C temperature. The weight loss rate is gradually increased with increase in temperature. In addition, the PBI copolymer-1 and PBI copolymer-2 were exhibited higher thermal stability than Nafion and acid doped PBI membranes. The Nafion membrane was degraded at 250 °C. Moreover, increased the temperature, it was sharply increased the loss of weight % and 18% recorded at 400 °C temperature, whereas; the acid doped PBI membranes weight lost 10 to 11 % only. Therefore, it is decided that the Nafion is unfavorable in high temperature operation. From the TGA curve, it is seen that the acid doped PBI membranes are stable until 175 °C temperature. In addition, both PBI membranes were a mutual thermal strength until 225 °C, later the PBI copolymer-1 showed little bit higher stability than PBI copolymer-2 membranes. Another interesting, whenever the temperature was crossed over 170°C, the orthophosphoric acid transforms into the pyrophosphoric acid.

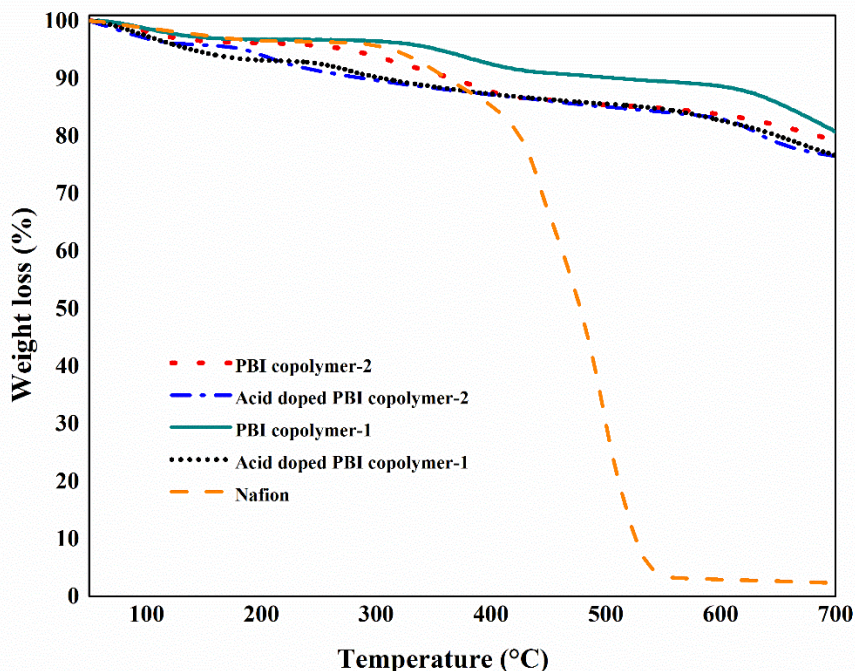


Figure 6. TGA curve of different solid electrolyte membranes.

To increase in temperature, it dries out the acid from the membrane, and this development continues up to 250°C. If the temperature rises to more than 250°C, then the membrane would go into thermal degradation. In contrast, the undoped membrane has more thermal stability than the H₃PO₄ acid doped membrane. From the aforementioned explanation, it may be concluded that the higher ADL of a membrane lowers the thermal stability to some extent. However, it is still good enough for working in the temperature range of 120 to 160°C, which is a promising factor for the high-temperature PEM fuel cell applications.

3.6 AFM images analysis

The surface roughness and topography of the polymer electrolyte membranes were studied by the AFM technique. The detailed surface feature of the Nafion, PBI copolymer-1 and PBI copolymer-2 membranes are shown in Figure 7. The average surface roughness (within 5 μm × 5 μm scan area) was found at 0.0036 μm, 0.0011 μm and 0.0088 μm for the Nafion, PBI copolymer-1 and PBI copolymer-2 membranes, respectively. Moreover, the average grain number was also counted at 55, 31 and 10 of the same scan area for the Nafion, PBI copolymer-1 and PBI copolymer-2 membranes, respectively. However, the grain and surface roughness of polymers were denoted the compatibility and the nature of interface between the crystals which may refer to the charge transfer resistance through the membrane. Therefore, it may assume that the ionic conductivity of polymer electrolyte has a correlation with the grain number and surface roughness of polymer electrolyte [43]. Moreover, the surface roughness may be enhanced the possibility of the hydrogen cross over from anode to cathode which reduced the open circuit voltage (OCV) of fuel cell [44].

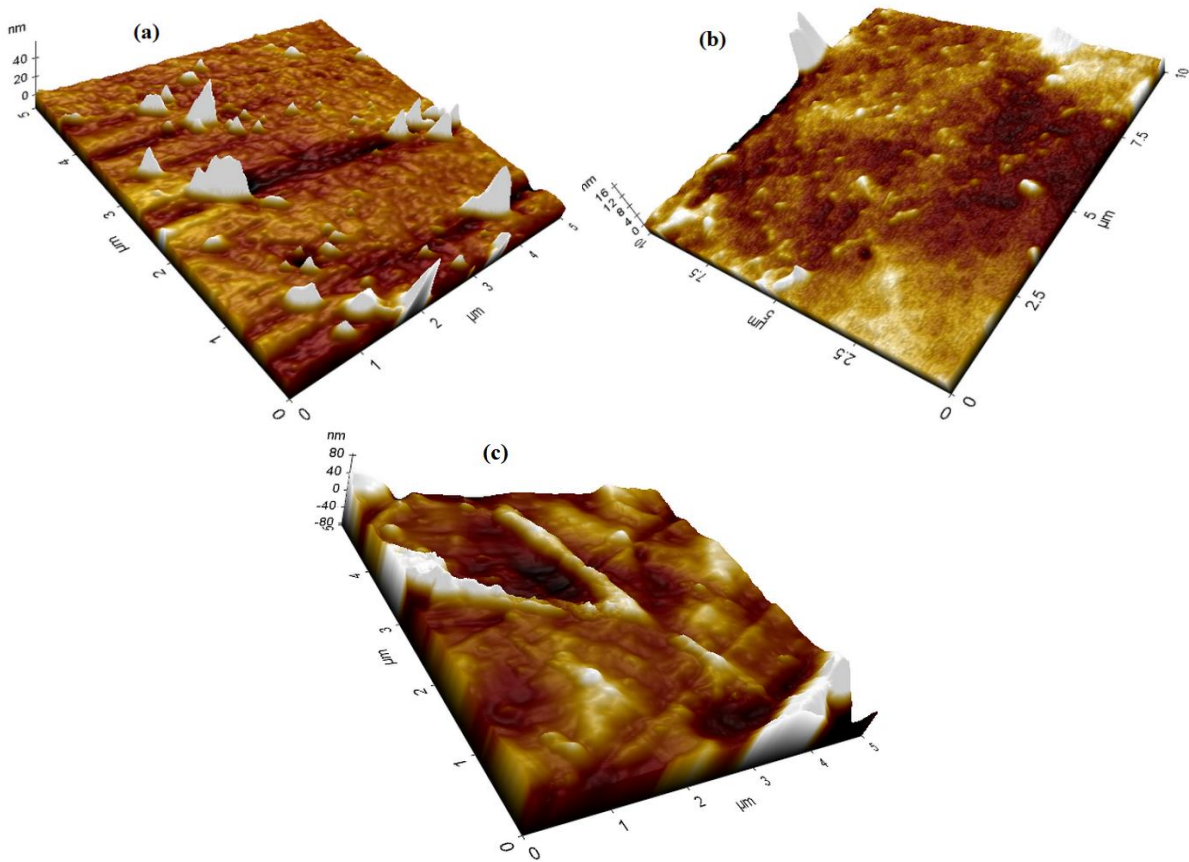


Figure 7. AFM images of (a) Nafion, (b) PBI copolymer-1 and (c) PBI copolymer-2 membranes.

3.7 FTIR analysis

The FTIR spectra of Nafion, PBI copolymer-1 and acid doped PBI copolymer-1 as well as PBI copolymer-2 and acid doped PBI copolymer-2 membranes are shown in Figure 8, respectively. According to the figure, major peaks of FTIR spectra were analyzed, and they subsequently detect the functional groups of Nafion, and also defined the phosphoric acid interaction inside the PBI copolymer-1 and PBI copolymer-2 membranes. In case of Nafion, several studies [13, 45, 46] were conducted that the IR spectra peaks were appeared at 1223 and 1155 cm^{-1} for C-F asymmetric and symmetric stretching, 1057 cm^{-1} for $-\text{SO}_3$ stretching, 983 cm^{-1} for C-O-C stretching and 526 cm^{-1} for $-\text{SO}_2\text{F}$ stretching frequencies, respectively.

Moreover, the major peaks were also appeared at 3464 and 1731 cm^{-1} due to the stretching of $-\text{OH}$ groups and water which represents the hydrogen bonding between the silanol, sulfonic groups of Nafion and water molecules. However, the peaks of pristine PBI copolymer-2 membrane were exhibited at 3626 and 3054 cm^{-1} for N—H group and stretching of hydrogen bonded N—H groups. In addition, the peaks were exhibited at 2035 cm^{-1} for aromatic carbon-hydrogen bond, 1614 cm^{-1} and 1538 cm^{-1} for C=N (double bond), as well as 1442 cm^{-1} and 1284 cm^{-1} indicated for C=C (double bond), respectively.

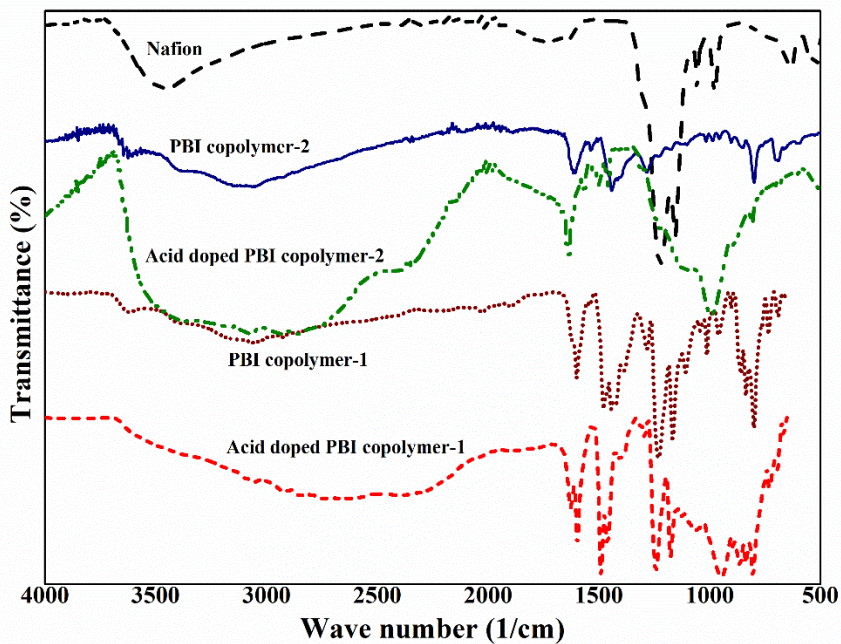


Figure 8. FTIR spectroscopy of solid electrolyte membranes.

P. H. Su [47] suggested that the undoped PBI copolymer-1 membrane was N—H and hydrogen bonded N—H groups that confirmed by the observed peaks at 3618 cm^{-1} and 3056 cm^{-1} , respectively. The stretching vibration of aromatic C—H groups was observed at 2028 cm^{-1} . The carbon-nitrogen double bond (C=N) peaks were appreciated at 1600 and 1541 cm^{-1} , whereas the peaks for carbon-carbon double bond (C=H) were observed at 1478 and 1445 cm^{-1} , respectively [48]. Later, acid doping of the PBI copolymer-1 membrane, the spectra were shifted and overlapped with the prior one. The phosphoric acid interacted with the membrane in the basic site of N—H groups that confirmed by the broad peak at 3057 to 2378 cm^{-1} . However, the carbon-nitrogen double bond (C=N) peaks were slightly shifted at 1627 and 1598 cm^{-1} . The peak was also shifted at 1490 and 1458 cm^{-1} for the carbon-carbon double bond (C=H). Moreover, S.W. Chuang [29] revealed that the peak for carbon-carbon (C—C) single bond of the PBI copolymer-1 membrane was observed at 1167 cm^{-1} . Finally, the phosphoric acid anions peak was appreciated at around 830 to 700 cm^{-1} .

3.8 Performance of single cell

The MEAs performance was investigated by the I-V polarization curves of the single cell of various solid polymer electrolytes as shown in Figure 9. Despite that, the active area was maintained at $5\text{ cm} \times 5\text{ cm}$ with the catalyst loading of MWCNT/Pt electrocatalyst at the anode side at $0.5\text{ mg}/\text{cm}^2$ and the cathode side at $0.7\text{ mg}/\text{cm}^2$. The MEAs were exhibited a distinctive trend which differentiated the MEAs performance according to their solid electrolyte membranes. The MEAs performance was measured by the fuel cell test station. Later, it can be drawn by the I-V polarization curves and power density curves of each MEAs.

Figure 9b shows the overall MEAs performance which conducted at 150 °C without using a humidifier. The PBI copolymer-1 based MEA was attributed maximum power density at 99.75 mW/cm² while, the PBI copolymer-2 based MEA and Nafion based MEA reported their power density at 85.19 mW/cm² and 68.46 mW/cm², respectively. Despite that, PBI is the better ionic conductive compared with the Nafion at high temperature. The cell resistance predominantly depends on the solid polymer electrolyte resistance. Moreover, three required processes and activities are involved in the PEMFC system; (i) proton conduction from anode to the cathode side through the membrane, (ii) electron transport from the current collector to the catalyst and contrariwise and (iii) the transport of gas reactants and product from catalyst layer to gas channel [49, 50].

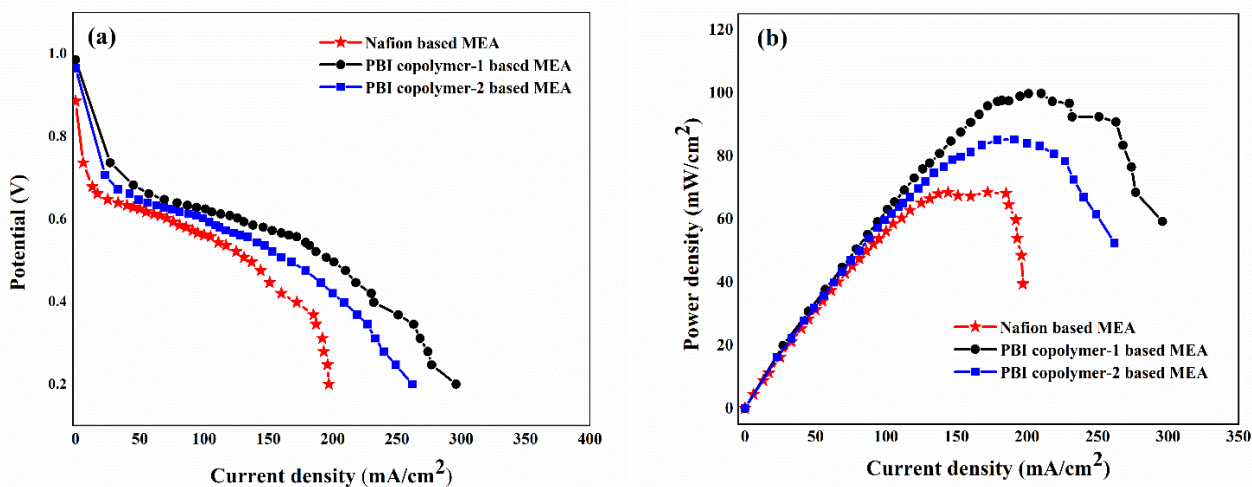


Figure 9. I-V Polarization curves (a) and power density curves (b) of MEAs at 150 °C temperature.

Although PBI and Nafion both are good ionomers which are promising for the PEMFC application. In contrast, the PBI is very effective at high temperature rather than the Nafion. Therefore, the PBI copolymer-1 based MEA is very effective under high operating temperature. Despite that, the PBI copolymer-1 based MEA was showed better performance than the PBI copolymer-2 based MEA due to the high proton conductivity. However, PBI copolymer-2 based MEA was also showed the positive trend at high temperature while the Nafion based MEA had a different trend.

4. CONCLUSIONS

This study reports that the PBI copolymer-1 is the most promising candidate for high-temperature PEM fuel cell application which based itself on the physiochemical characteristics. The proton conductivity was measured at 5.29 mS/cm, 6.52 mS/cm and 5.69 mS/cm under different temperature of PBI copolymer-1, PBI copolymer-2, and Nafion membranes, respectively. Based on this results, it was significantly depended on the operating temperatures. In addition, the PBI copolymer-1 membrane was shown better chemical and mechanical strength which endorsed by the Fenton test and stress-strain

curve. However, TGA curves were demonstrated that the PBI membrane had excellent thermal resistance at high temperature, which reveals window as polymer electrolyte membrane for future high-temperature PEM fuel cell applications.

ACKNOWLEDGEMENT

This research was supported by the Universiti Kebangsaan Malaysia under the Grant AP-2013-010. The authors are very thankful to the Universiti Kebangsaan Malaysia administrations for their financial support.

References

1. K. Sopian, and W. R. W. Daud, *Renew. Energy*, 31 (2006) 719.
2. R. E. Rosli, A. B. Sulong, W. R. W. Daud, M. A. Zulkifley, T. Husaini, M. I. Rosli, E. H. Majlan, and M. A. Haque, *Int. J. Hydrogen Energy*, 42 (2017) 9293.
3. Z. Tang, H. Y. Ng, J. Lin, A. T. Wee, and D. H. Chua, *J. Electrochem. Soc.*, 157 (2010) 245.
4. Y. Shao, G. Yin, Y. Gao, and P. Shi, *J. Electrochem. Soc.*, 153 (2006) 1093.
5. F. Lufrano, V. Baglio, P. Staiti, A. S. Arico, and V. Antonucci, *Desalination*, 199 (2006) 283.
6. C. Wieser, *Fuel Cells*, 4 (2004) 245.
7. H. Zhang, and P. K. Shen, *Chem. Rev.*, 112 (2012) 2780.
8. J. Jouanneau, R. Mercier, L. Gonon, and G Gebel, *Macromolecules*, 40 (2007) 983.
9. B. Xing, and O. Savadogo, *J. New Mat. Electrochem. Syst.*, 2 (1999) 95.
10. M. A. Haque, A. B. Sulong, K. S. Loh, E. H. Majlan, T. Husaini, and R. E. Rosli, *Int. J. Hydrogen Energy*, 42 (2017) 9156.
11. H. Y. Chang, and C. W. Lin, *J. Membr. Sci.*, 218 (2003) 295.
12. H. Y. Chang, R. Thangamuthu, and C. W. Lin, *J. Membr. Sci.*, 228 (2004) 217.
13. T. Navessin, M. Eikerling, Q. Wang, D. Song, Z. Liu, J. Horsfall, and S. Holdcroft, *J. Electrochem. Soc.*, 152 (2005) 796.
14. H. S. Thiam, W. R. W. Daud, S. K. Kamarudin, A. B. Mohamad, A. A. Kadhum, K. S. Loh, and E. H. Majlan, *Int. J. Hydrogen Energy*, 38 (2013) 9474.
15. J. Wang, H. Zhang, Z. Jiang, X. Yang, L. Xiao, *J. Power Sources*, 188 (2009) 64.
16. S. Kang, C. Zhang, G. Xiao, D. Yan, G. Sun, *J. Membr. Sci.*, 334 (2009) 91.
17. J. B. Wagner, and C. Wagner, *J. Chem. Phys.*, 26 (1957) 1597.
18. Q. Li, J. O. Jensen, R. F. Savinell, and N. J. Bjerrum, *Prog. Polym. Sci.*, 34 (2009) 449.
19. Q. Li, C. Pan, J. O. Jensen, P. Noyé, and N. J. Bjerrum, *Chem. Mater.*, 19 (2007) 350.
20. J. S. Yang, L. N. Cleemann, T. Steenberg, C. Terkelsen, Q. F. Li, J. O. Jensen, and R. H. He, *Fuel Cells*, 14 (2014) 7.
21. E. L. Strauss, *Polym. Eng. Sci.*, 6 (1966) 24.
22. F. Mack, M. Klages, J. Scholte, L. Jörissen, T. Morawietz, R. Hiesgen, R. Zeis, *J. Power Sources*, 255 (2014) 431.
23. M. Jaffe, M. Haider, J. Menczel, and J. Rafalko, *Polym. Eng. Sci.*, 32 (1992) 1236.
24. E. H. Majlan, D. Rohendi, W. R. W. Daud, T. Husaini, and M. A. Haque, *Renew. Sust. Energ. Rev.* 89 (2018) 117.
25. R. E. Rosli, A. B. Sulong, W. R. W. Daud, M. A. Zulkifley, T. Husaini, M. I. Rosli, E. H. Majlan, and M. A. Haque, and N. A. M. Radzuan, *Int. J. Hydrogen Energy*, (2018).
26. S. Y. Toh, K. S Loh, S. K. Kamarudin, and W. R. W. Daud, *Electrochim. Acta* 199 (2016) 194.
27. M. A. Haque, A. B. Sulong, K. S. Loh, E. H. Majlan, T. Husaini, R. E. Rosli, and M. A. A. Mashud, *WIECON-ECE*, (2015) 552.

28. J. X. Leong, W. R. W. Daud, M. Ghasemi, A. Ahmad, M. Ismail, and K. B. Liew, *Int. J. Hydrogen Energy*, 40 (2015) 11604.
29. S. W. Chuang, S. L. C. Chuang, Hsu, and M. L. Yang, *Eur. Polym. J.*, 44 (2008) 2202.
30. Q. Li, R. He, J. Jensen, and N. Bjerrum, *Fuel Cells*, 4 (2004) 147.
31. J. A. Asensio, S. Borrós, and P. Gómez-Romero, *J. Membr. Sci.*, 241 (2004) 89.
32. J. Parrondo, C. R. Venkateswara, S. L. Ghatty, and B. Rambabu, *Int. J. Electrochem.*, (2010) 2011
33. M. Q. Li, Z. G. Shao, and K. Scott, *J. Power Sources*, 183 (2008) 69.
34. A. L. Ong, G. B. Jung, C. C. Wu, and W. M. Yan, *Int. J. Hydrogen Energy*, 35 (2010) 7866.
35. L. Qingfeng, H. A. Hjuler, and N. Bjerrum, *J. Appl. Electrochem.*, 31 (2001) 773.
36. J. W. Lee, D. Y. Lee, H. J. Kim, S. Y. Nam, J. J. Choi, J. Y. Kim, J. H. Jang, E. Cho, S. K. Kim, S. A. Hong, *J. Membr. Sci.*, 357 (2010) 130.
37. T. H. Kim, T. W. Lim, and J. C. Lee, *J. Power Sources*, 172 (2007) 172.
38. J. S. Yang, L. N. Cleemann, T. Steenberg, C. Terkelsen, Q. F. Li, J. O. Jensen, and R. H. He, *Fuel Cells*, 14 (2014) 7.
39. L. Xiao, H. Zhang, T. Jana, E. Scanlon, R. Chen, E. W. Choe, and B. C. Benicewicz, *Fuel Cells*, 5 (2005) 287.
40. C. Wannek, W. Lehnert, and J. Mergel, *J. Power Sources*, 192 (2009) 258.
41. J. Wu, X.Z. Yuan, J. J. Martin, H. Wang, J. Zhang, J. Shen, and W. Merida, *J. Power Sources*, 184 (2008) 104.
42. J. Liao, J. Yang, Q. Li, L. N. Cleemann, J. O. Jensen, N. J. Bjerrum, and W. Xing, *J. Power Sources*, 238 (2013) 516.
43. Y. S. Kim, L. Dong, M. A. Hickner, B. S. Pivovar, J.E. McGrath, *Polymer*, 44 (2003) 5729.
44. K. D Baik, S. I. Kim, B. K. Hong, K. Han, and M. S. Kim. *Int. J. Hydrogen Energy*, 36 (2011) 9916.
45. Y. Wei, L. Shen, Z. Wang, W. D. Yang, H. Zhu, and H. Liu, *Int. J. Hydrogen Energy*, 36 (2011) 5088.
46. H. Li, M. Ai, F. Jiang, L. Yu, H. Tu, Q. Yu, and H. Wang, *J. Power Sources*, 196 (2011) 4583.
47. P. H. Su, J. Cheng, J. F. Li, Y. H. Liao, and T. L. Yu, *J. Power Sources*, 260 (2014) 131.
48. S. Seodaemun-gu, *Int. J. Electrochem. Sci.*, 7 (2012) 6276.
49. H. Kim, N. P. Subramanian, B. N. Popov, *J. Power Sources*, 138 (2004) 14.
50. H. N. Su, S. J. Liao, T. Shu, and H. L. Gao, *J. Power Sources*, 195 (2010) 756.